Rényi Entropy for Heterogeneity Identification in SAR Data

J. Alpala

We present a statistical method for identifying roughness characteristics in synthetic aperture radar (SAR) intensity data through the use of Rényi entropy. Homogeneous regions, characterized by fully-developed speckle, are modeled with the Gamma distribution, while heterogeneous areas are described by the G_I^0 distribution, where fully-developed speckle assumptions do not apply. Our proposed hypothesis test, based on a non-parametric estimator of Renyi entropy, effectively distinguishes between homogeneous and heterogeneous regions. Results indicate that the Rényi entropy-based approach provides superior performance compared to previous methods using Shannon entropy, offering enhanced detection of heterogeneity in both simulated and real SAR data.

Keywords: Gamma distribution, heterogeneity, SAR, Rényi entropy, hypothesis tests

Introduction

Synthetic Aperture Radar (SAR) technology is a powerful tool for environmental monitoring and disaster management, providing valuable imagery in all weather conditions, day or night Moreira et al. (2013); Mu et al. (2019). However, effective use of SAR data requires a thorough understanding of its statistical properties due to the presence of speckle, an interference effect inherent in SAR data caused by the coherent nature of the imaging process Argenti et al. (2013).

To model SAR intensity data, the $\mathcal{G}^0$ distribution is commonly used, as it provides flexibility for representing different levels of roughness, with the Gamma distribution serving as a limiting case for homogeneous regions with fully-developed speckle De A. Ferreira and Nascimento (2020). Our goal is to improve the identification of roughness features in SAR intensity data by employing Rényi entropy as a new tool for distinguishing between homogeneous and heterogeneous regions.

Entropy is a fundamental concept in information theory, applied in various fields such as image processing, statistical physics, and SAR image analysis Pressé et al. (2013); Mohammad-Djafari (2015); Avval et al. (2021); Nascimento et al. (2014); Nascimento, Frery and Cintra (2019). Originally introduced by Shannon in 1948 Shannon (1948), entropy measures information and uncertainty in a random variable. In this work, we utilize Rényi entropy, which generalizes Shannon entropy and provides a different perspective on data dispersion, particularly suited for SAR data.

We propose a hypothesis test based on a non-parametric estimator of Rényi entropy to distinguish between homogeneous and heterogeneous regions. This approach is more effective than previous methods based on Shannon entropy, offering improved detection capabilities. Our proposed method is applied to generate homogeneity maps that reveal various target types in SAR data, demonstrating superior performance with both simulated and real SAR images.

The article is structured as follows: Section discusses statistical modeling and entropy estimation for intensity SAR data. Section outlines the hypothesis tests based on non-parametric entropy estimators. In Section **??**, we present experimental results. Finally, Section **??** provides conclusions.

Background

Statistical Modeling of Intensity SAR data

The primary models for intensity SAR data include the Gamma and $\mathcal{G}_I^0$ distributions (Frery et al., 1997). The first is suitable for fully-developed speckle and is a limiting case of the second model. This is interesting due to its versatility in accurately representing regions with different roughness properties(Cassetti et al., 2022). We denote $Z \sim \Gamma_{\text{SAR}}(L,\mu)$ and $Z \sim \mathcal{G}_I^0(\alpha,\gamma,L)$ to indicate that Z follows the distributions characterized by the respective probability density functions (pdfs):

$$f_Z(z; L, \mu \mid \Gamma_{\text{SAR}}) = \frac{L^L}{\Gamma(L)\mu^L} z^{L-1} \exp\left\{-Lz/\mu\right\} \mathbb{1}_{\mathbb{R}_+}(z) \tag{1}$$

and

$$f_Z(z; \alpha, \gamma, L \mid \mathcal{G}_I^0) = \frac{L^L \Gamma(L-\alpha)}{\gamma^\alpha \Gamma(-\alpha)\Gamma(L)} \cdot \frac{z^{L-1}}{(\gamma + Lz)^{L-\alpha}} \mathbb{1}_{\mathbb{R}_+}(z), \tag{2}$$

where $\mu > 0$ is the mean, $\gamma > 0$ is the scale, $\alpha < 0$ measures the roughness, $L \geq 1$ is the number of looks (either nominal or estimated, thus not restricted to integer values), $\Gamma(\cdot)$ is the gamma function, and $\mathbb{1}_A(z)$ is the indicator function of the set A.

The rth order moments of the $\mathcal{G}_I^0$ model are

$$E\big(Z^r \mid \mathcal{G}_I^0\big) = \left(\frac{\gamma}{L}\right)^r \frac{\Gamma(-\alpha - r)}{\Gamma(-\alpha)} \cdot \frac{\Gamma(L+r)}{\Gamma(L)}, \tag{3}$$

provided $\alpha < -r$, and infinite otherwise. Therefore, assuming $\alpha < -1$, its expected value is

$$\mu = \left(\frac{\gamma}{L}\right) \frac{\Gamma(-\alpha - 1)}{\Gamma(-\alpha)} \cdot \frac{\Gamma(L+1)}{\gamma(L)} = -\frac{\gamma}{\alpha + 1}. \tag{4}$$

Although the $\mathcal{G}_I^0$ distribution is defined by the parameters α and γ, in the SAR literature Nascimento, Cintra and Frery (2010) the texture α and the mean μ are usually used. Reparametrizing (2) with μ, and denoting this model as G_I^0 we obtain:

$$f_Z\big(z; \mu, \alpha, L \mid G_I^0\big) = \frac{L^L \Gamma(L-\alpha)}{\big[-\mu(\alpha+1)\big]^\alpha \Gamma(-\alpha)\Gamma(L)} \frac{z^{L-1}}{\big[-\mu(\alpha+1) + Lz\big]^{L-\alpha}}. \tag{5}$$

Rényi Entropy

Introduced by Alfréd Rényi in 1961, the Rényi entropy generalizes several entropy measures, including the Shannon entropy. For a continuous random variable Z with probability density function (pdf) $f(z)$, the Rényi entropy of order λ (where $\lambda > 0$ and $\lambda \neq 1$) is defined as:

$$H_\lambda(Z) = \frac{1}{1-\lambda} \ln \int_{-\infty}^{\infty} [f(z)]^\lambda \, dz. \tag{6}$$

Using this definition, we obtain the Rényi entropy expressions for the Γ_{SAR} and G_I^0 distributions, respectively:

$$H_\lambda(\Gamma_{\text{SAR}}) = \frac{1}{\lambda-1}\left[\lambda\,\ln\Gamma(L) - \ln\Gamma\big(\lambda(L-1)+1\big) - (\lambda-1)\big(\ln L - \ln\mu\big) + \big(\lambda(L-1)+1\big)\,\ln\lambda\right]. \tag{7}$$

$$\begin{aligned} H_\lambda(G_I^0) &= \ln\mu + \ln(-1-\alpha) - \ln L \\ &+ \frac{1}{1-\lambda}\left[\lambda\left(\ln\Gamma(L-\alpha) - \ln\Gamma(-\alpha) - \ln\Gamma(L)\right) + \ln\Gamma\left(\lambda(L-1)+1\right) + \ln\Gamma\left(\lambda(-\alpha+1)-1\right) - \ln\Gamma\left(\lambda(L-\alpha)\right)\right]. \end{aligned} \tag{8}$$

Appendix provides the detailed derivations of the Rényi entropy for both the Γ_{SAR} and G_I^0 distributions.

Figure 1, shows the entropy of G_I^0 as a function of μ when $\alpha \in \{-\infty, -20, -8, -3\}$. Notice that it converges to the entropy of Γ_{SAR} when $\alpha \to -\infty$, as expected.

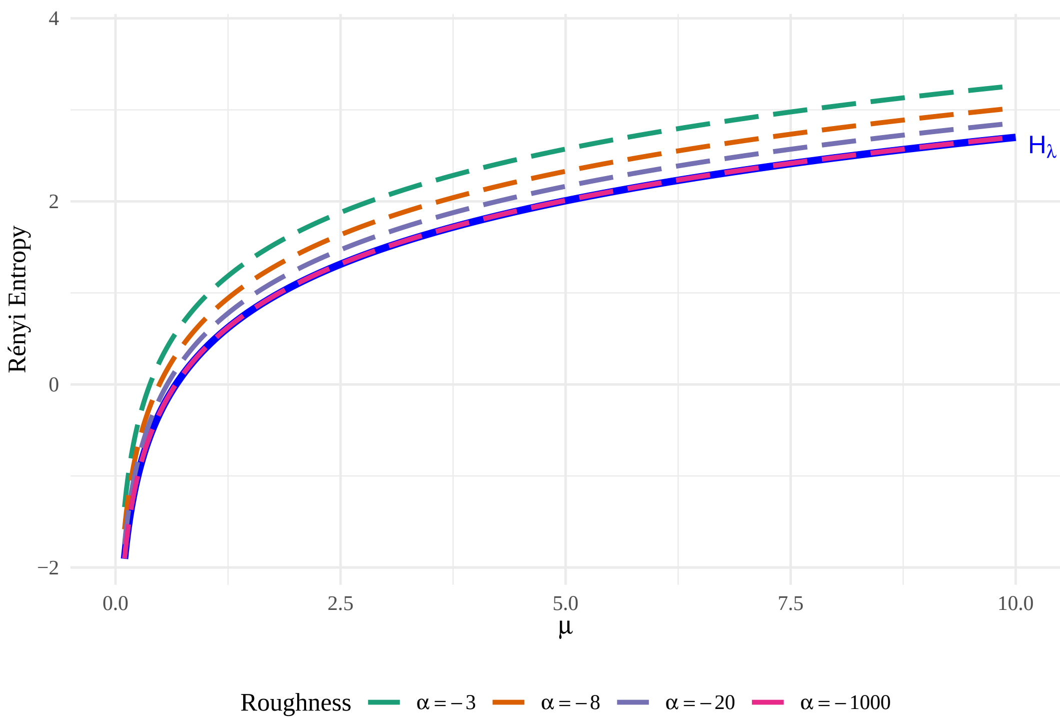

Figure 1: $H_{G_I^0}$ converges to the $H_{\Gamma_{\text{SAR}}}$ when $\alpha \to -\infty$, with $L = 8$.

Estimation of Rényi Entropy

Consider a sample $Z_1, Z_2, \ldots, Z_n$ drawn from the distribution F. Let $Z_{(1)} \leq Z_{(2)} \leq \cdots \leq Z_{(n)}$ represent the order statistics of $Z_1, Z_2, \ldots, Z_n$. The density estimator based on m spacing, introduced by Vasicek (1976) and extended by Ebrahimi et al. (1994), is given by:

$$f_n(Z_{(i)}) = \frac{c_i m/n}{Z_{(i+m)} - Z_{(i-m)}},$$

where $Z_{(i-m)} = Z_{(1)}$ if $i \leq m$ and $Z_{(i+m)} = Z_{(n)}$ if $i \geq n-m$, and c_i is defined as:

$$c_i = \begin{cases} \frac{m+i-1}{m}, & \text{if } 1 \leq i \leq m, \\ 2, & \text{if } m+1 \leq i \leq n-m, \\ \frac{n+m-i}{m}, & \text{if } n-m+1 \leq i \leq n. \end{cases}$$

We begin by estimating $H_\lambda(F)$, as defined in the general form of the Rényi entropy. Note that $H_\lambda(F)$ can be expressed as:

$$H_\lambda(F) = \frac{1}{1-\lambda} \log \int_S (f(x))^{\lambda-1} dF(x) = \frac{1}{1-\lambda} \log \int_0^1 \left(\frac{d}{dt} F^{-1}(t) \right)^{1-\lambda} dt.$$

Following Vasicek (1976) and Ebrahimi et al. (1994) for the estimation of Shannon entropy and utilizing $f_n(Z_{(i)})$ from the previous equation, $H_\lambda(F)$ can be estimated by:

$$\hat{H}_\lambda(\boldsymbol{Z}) = \frac{1}{1-\lambda} \log \left(\frac{1}{n} \sum_{i=1}^{n} \left(\frac{c_i m/n}{Z_{(i+m)} - Z_{(i-m)}} \right)^{\lambda-1} \right).$$

This estimator allows for the estimation of the Rényi entropy in a non-parametric framework.

Enhanced estimators with Bootstrap

We use the bootstrap technique to refine the accuracy of non-parametric entropy estimators. In this approach, new data sets are generated by replicate sampling from an existing data set Michelucci and Venturini (2021).

Let us assume that the non-parametric entropy estimator $\widehat{H} = \widehat{\theta}(\boldsymbol{Z})$ is inherently biased, i.e,:

$$\text{Bias}\left(\widehat{\theta}(\boldsymbol{Z})\right) = E\big[\widehat{\theta}(\boldsymbol{Z})\big] - \theta \neq 0. \tag{9}$$

Our bootstrap-improved estimator is of the form:

$$\widetilde{H} = 2\widehat{\theta}(\boldsymbol{Z}) - \frac{1}{B} \sum_{b=1}^{B} \widehat{\theta}_b(\boldsymbol{Z}^{(b)}),$$

where B is the number of observations obtained by resampling from $\boldsymbol{Z}$ with replacement.

Optimal λ for $n = 49$

We aim to determine the optimal order λ for the Rényi entropy estimator, specifically for a sample size of $n = 49$. To identify this optimal value, we analyze both the Mean Squared Error (MSE) and Bias of the estimator across different values of λ. Lower MSE and Bias indicate better performance of the estimator in approximating the true entropy.

Based on the results, we find that the optimal value of λ is 0.9, as it minimizes the MSE while maintaining a low Bias, as shown in Figure 2.

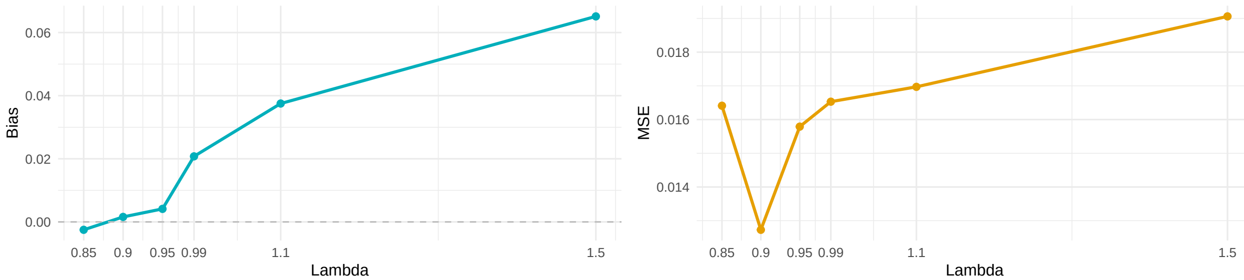

Figure 2: Bias as a function of λ, with $n = 49$, $L = 5$.

We analyzed the performance of these estimators with a Monte Carlo study: 1000 samples from the Γ_{SAR} distribution of size $n \in \{9, 25, 49, 81, 121\}$, with $\mu = 10$ and $L = 5$. The choice of $\lambda = 0.9$ is consistent with findings in other scenarios. We used $B = 200$ bootstrap samples and the heuristic spacing $m = [\sqrt{n} + 0.5]$, as recommended in the literature.

In Figure 3, we show the bias and mean squared error (MSE) of the non-parametric entropy estimator and their respective bootstrap-enhanced version. The bootstrap-enhanced estimator demonstrate smaller bias and MSE, reinforcing their effectiveness in providing more reliable entropy estimates.

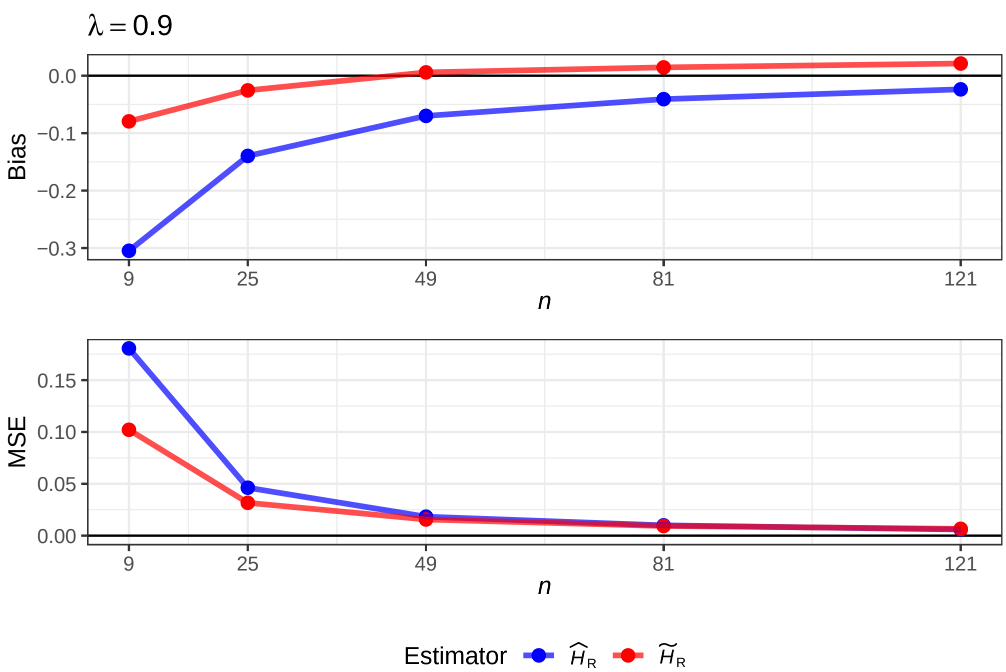

Figure 3: Bias and MSE of the Rényi entropy estimators for the Γ_{SAR}, with $\lambda = 0.9$, $\mu = 10$ and $L = 5$.

Hypothesis Testing

We aim to test the following hypotheses:

$$\begin{cases} \mathcal{H}_0: & \text{The data come from the } \Gamma_{\text{SAR}} \text{ law,} \\ \mathcal{H}_1: & \text{The data come from the } G_I^0 \text{ distribution.} \end{cases}$$

We are testing the hypothesis that the data are fully-developed speckle versus the alternative of data with roughness. As for the parametric problem, once it is not possible to define the hypothesis $\mathcal{H}_0 = \alpha = -\infty$, it is impossible to solve this problem with parametric inference alternatives (such as likelihood ratio, score, gradient, and Wald hypothesis test). The proposed tests to solve this physical problem in SAR systems are described below.

The Proposed Test Based on Non-parametric Entropy

For a random sample $\boldsymbol{Z} = (Z_1, Z_2, \dots, Z_n)$ from a distribution $\mathcal{D}$, a test statistic is proposed. It is based on an empirical distribution that arises from the difference between non-parametrically estimated entropies $\widetilde{H}(\boldsymbol{Z})$ and the analytical entropy of Γ_{SAR} (**??**) evaluated at the logarithm of the sample mean, where $L \geq 1$ is known.

Hence, the entropy-based test statistic is defined as:

$$S(\boldsymbol{Z}; L) = \widetilde{H}(\boldsymbol{Z}) - \left[H_{\Gamma_{\text{SAR}}}(L) + \ln \overline{\boldsymbol{Z}}\right]. \tag{10}$$

This test statistic aims to assess the behavior of the data under the null hypothesis using the empirical distribution. If the data represent fully-developed speckle, the density should center around zero, i.e., $S(\boldsymbol{Z}; L) \approx 0$. Otherwise, the empirical distribution would shift from zero under the alternative hypothesis, suggesting significant differences and heterogeneous clutter.

We now verify the normality of the data generated by the $S_{\widetilde{H}_{\text{R}}}(\boldsymbol{Z}; L)$ test. Figure 4 shows the empirical densities obtained by applying the test to different sample sizes drawn from the Γ_{SAR} distribution, where L takes values $\{3, 5, 18, 36\}$ and $\mu = 1$. Additionally, Table 1 summarizes the main descriptive statistics, including mean, standard deviation (SD), variance (Var), skewness (SK), excessive kurtosis (EK) and Anderson–Darling p values for normality. Results with p values greater than 0.05 do not indicate a violation of the normality assumption. A low variance, skewness, and excessive kurtosis of almost zero indicate limited dispersion, asymmetry, and a light tail. Normal Q–Q plots confirm no evidence against a normal distribution, as shown in Figure 5.

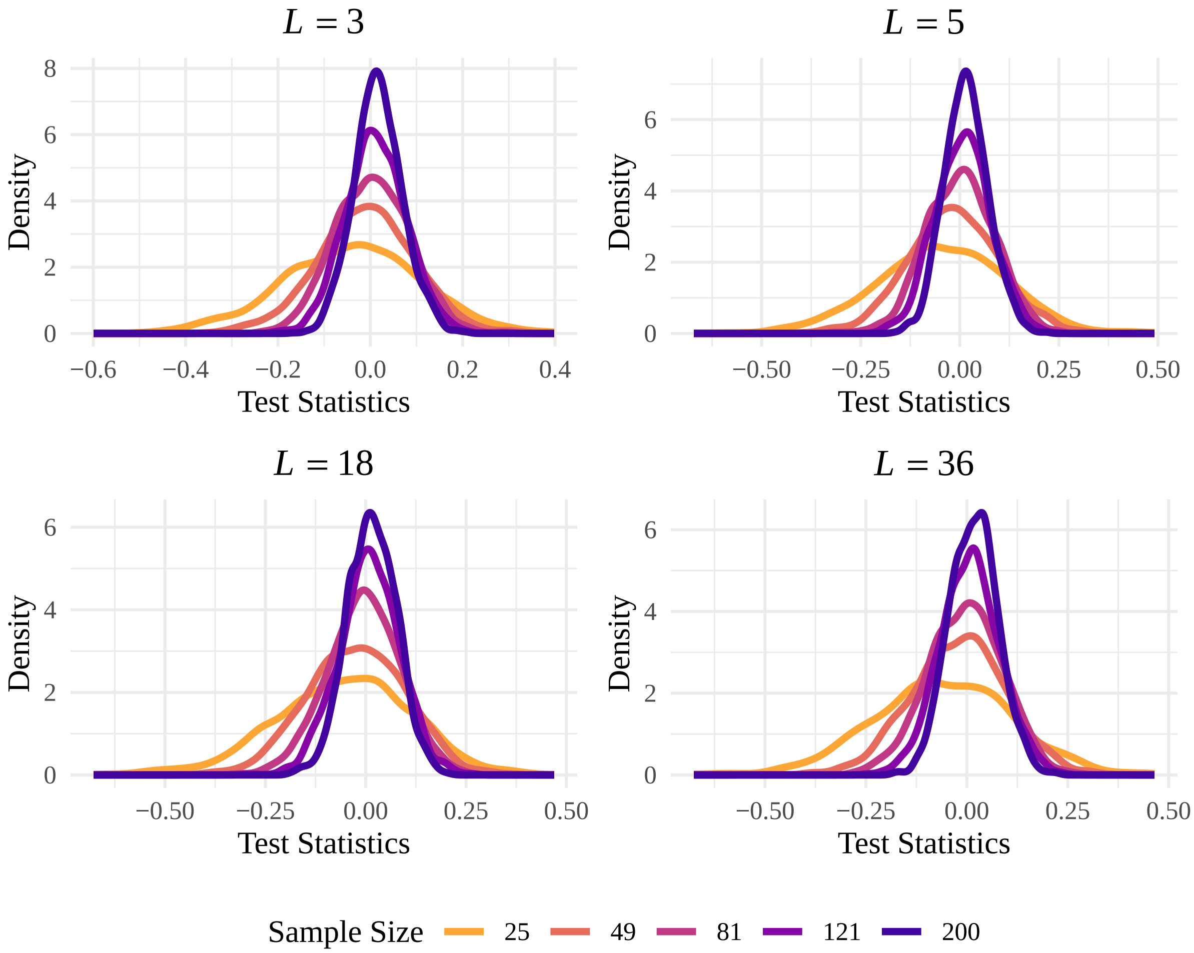

Figure 4: Empirical densities obtained from $S_{\widetilde{H}_{\mathrm{R}}}(\boldsymbol{Z};L)$ test under the null hypothesis, with $\lambda = 0.8$ and $\mu = 10$.

Table 1: Descriptive analysis of $S_{\widetilde{H}_{\mathrm{R}}}(\boldsymbol{Z}; L)$, with $L \in \{3, 5, 18, 36\}$ and $\mu = 10$.

L	n	Mean	SD	Var	SK	EK	p-value
3	25	-0.0419	0.1483	0.0220	-0.0988	-0.0325	0.1699
	49	-0.0101	0.1049	0.0110	-0.0378	0.1756	0.3470
	81	0.0040	0.0811	0.0066	0.0632	0.1027	0.4084
	121	0.0119	0.0659	0.0043	0.0618	0.1396	0.6906
	200	0.0170	0.0528	0.0028	0.1579	0.1517	0.0091
5	25	-0.0471	0.1604	0.0257	-0.0979	0.1507	0.1691
	49	-0.0170	0.1135	0.0129	-0.0614	0.1442	0.8241
	81	0.0009	0.0856	0.0073	-0.0710	0.0131	0.3801
	121	0.0076	0.0706	0.0050	0.0042	-0.0536	0.4890
	200	0.0160	0.0558	0.0031	0.1141	0.0912	0.0940
18	25	-0.0555	0.1683	0.0283	-0.2520	0.1535	0.0002
	49	-0.0235	0.1212	0.0147	-0.0460	-0.1341	0.3318
	81	-0.0053	0.0904	0.0082	-0.1230	-0.0410	0.2344
	121	0.0088	0.0759	0.0058	-0.0782	0.1803	0.0612
	200	0.0153	0.0610	0.0037	-0.0612	-0.0385	0.2884
36	25	-0.0608	0.1693	0.0287	-0.1020	0.1121	0.1869
	49	-0.0208	0.1175	0.0138	-0.1283	0.1795	0.1427
	81	-0.0040	0.0918	0.0084	-0.0861	-0.1464	0.2691
	121	0.0072	0.0743	0.0055	0.0065	0.0237	0.7377
	200	0.0169	0.0601	0.0036	0.0476	-0.0207	0.4091

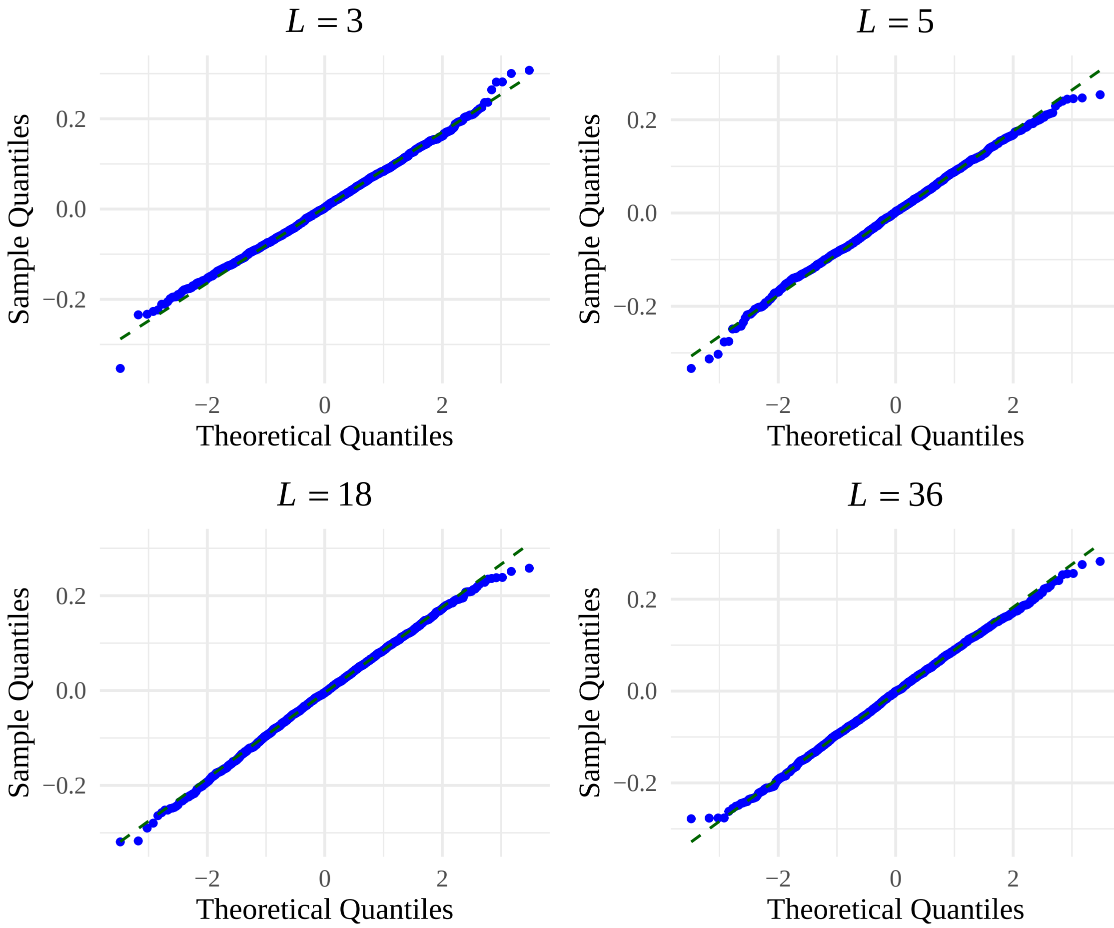

Figure 5: Normal Q–Q plots for $n = 81$. The dashed green lines in the Q–Q plots represent theoretical expected quantiles for a normal distribution. Variations in the scales of the axes reflect differences in the range of values across datasets.

We also evaluated the test's power by performing 1000 simulations under the alternative hypothesis (G_I^0 distribution) with $\mu = 1$ and $\alpha = -2$. The power generally improves with increasing sample size and number of looks. The results are shown in Table 2.

Table 2: Size and Power of the $S_{\widetilde{H}_{\mathrm{R}}}(\boldsymbol{Z})$ test statistic.

		Size			Power		
$\boldsymbol{L}$	$\boldsymbol{n}$	**1%**	**5%**	**10%**	**1%**	**5%**	**10%**
5	25	0.0140	0.0500	0.1000	0.9780	0.9940	0.9930
	49	0.0110	0.0480	0.1090	0.9940	1.0000	0.9990
	81	0.0120	0.0570	0.1030	0.9980	0.9980	0.9990
	121	0.0130	0.0610	0.1160	0.9990	0.9990	0.9970
8	25	0.0100	0.0510	0.1050	0.9960	0.9990	1.0000
	49	0.0080	0.0560	0.1090	1.0000	0.9990	1.0000
	81	0.0120	0.0520	0.0970	0.9990	0.9990	0.9990
	121	0.0160	0.0700	0.1160	0.9980	1.0000	0.9990
18	25	0.0160	0.0510	0.1110	1.0000	1.0000	1.0000
	49	0.0140	0.0470	0.0980	1.0000	1.0000	1.0000
	81	0.0130	0.0480	0.1060	1.0000	1.0000	1.0000
	121	0.0120	0.0660	0.1100	1.0000	1.0000	1.0000

Results

This section presents the simulations we performed to evaluate the proposed test statistics' performance, followed by applications to SAR data.

Simulated Data

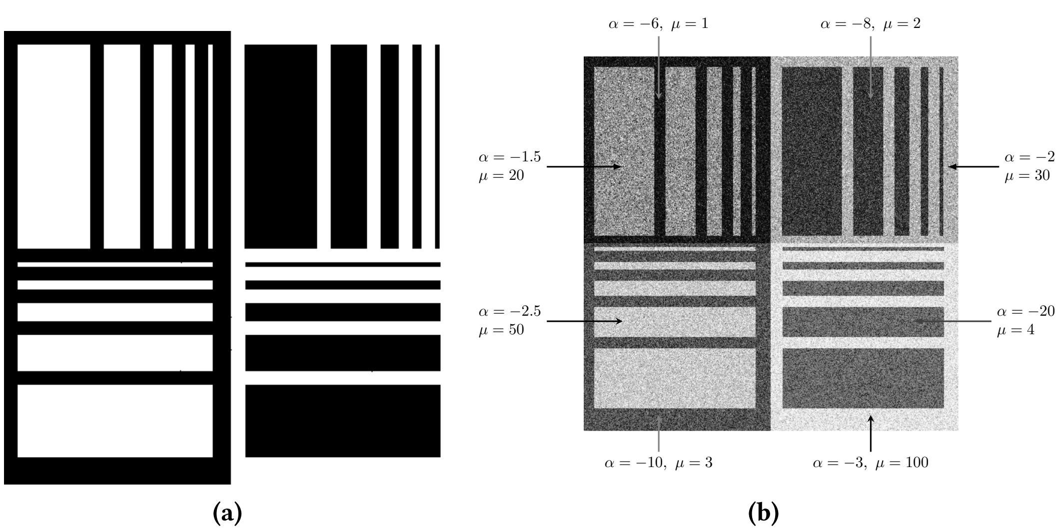

Figure 6: Synthetic dataset: (**a**) Phantom. (**b**) Simulated image, varying α and μ, with $L = 5$.

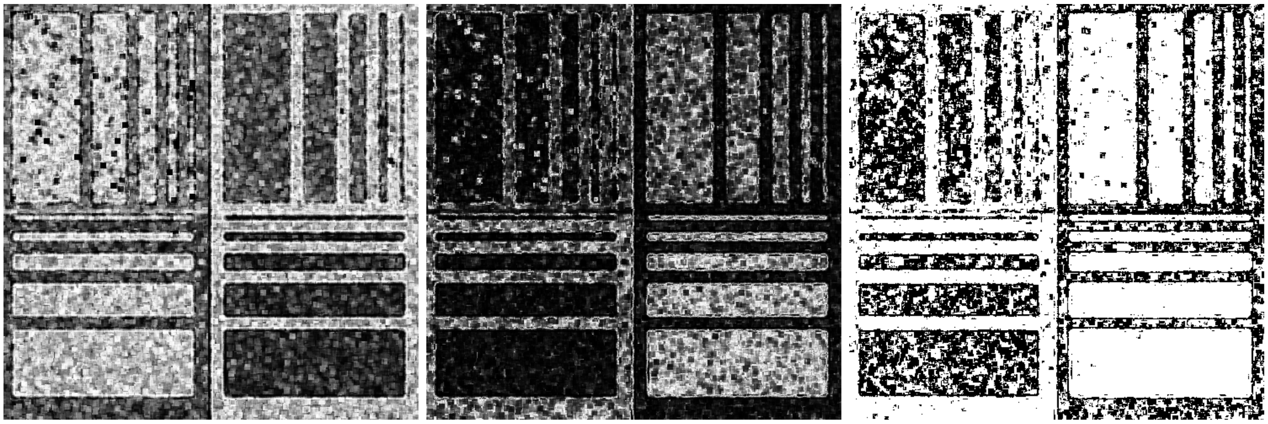

(a) **(b)** **(c)**

Figure 7: Results for a threshold of 0.05 of the p-value, Shannon entropy, $L = 5$.

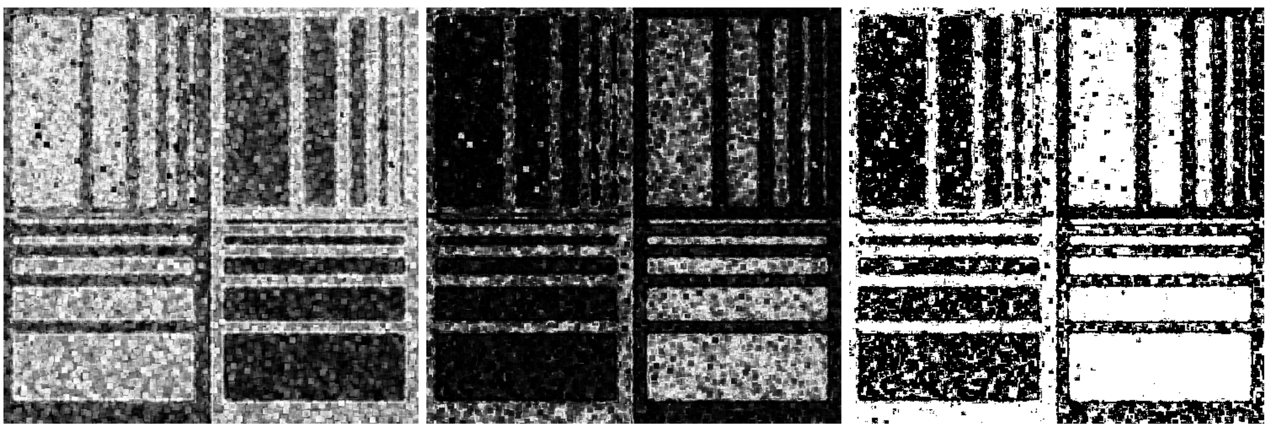

(a) **(b)** **(c)**

Figure 8: Results for a threshold of 0.05 of the p-value, Rényi Entropy, $L = 5$, $\lambda = 0.9$, $n = 49$.

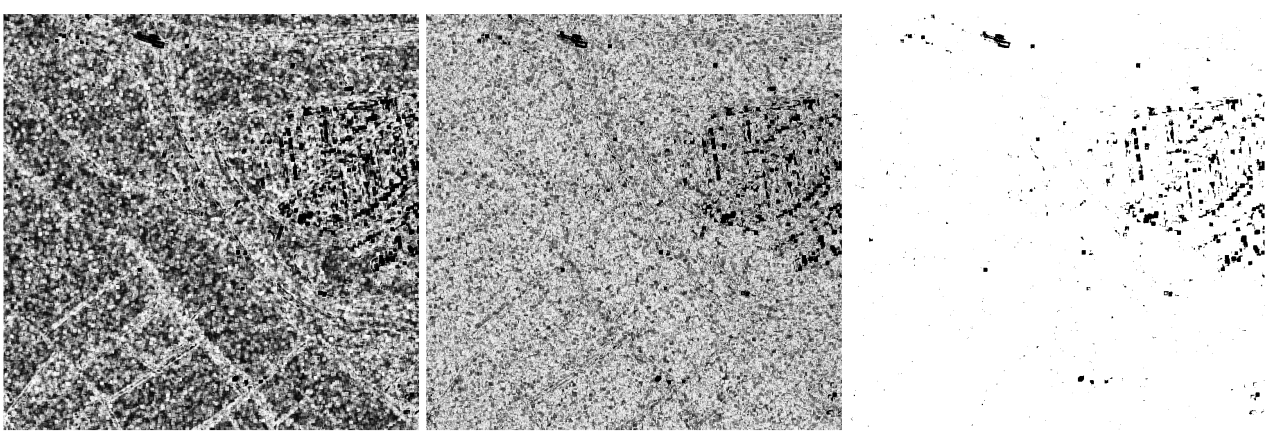

(a) **(b)** **(c)**

Figure 9: Results for a threshold of 0.05 of the p-value, Shannon entropy, $L = 1$.

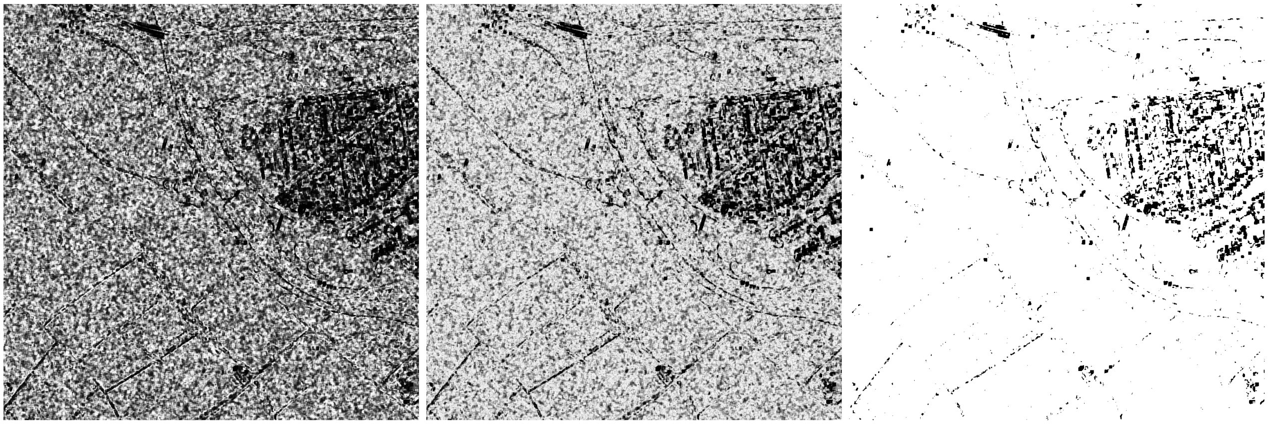

(a) **(b)** **(c)**

Figure 10: Results for a threshold of 0.05 of the p-value, Rényi Entropy, $L = 1$, $\lambda = 2.0$, $n = 49$.

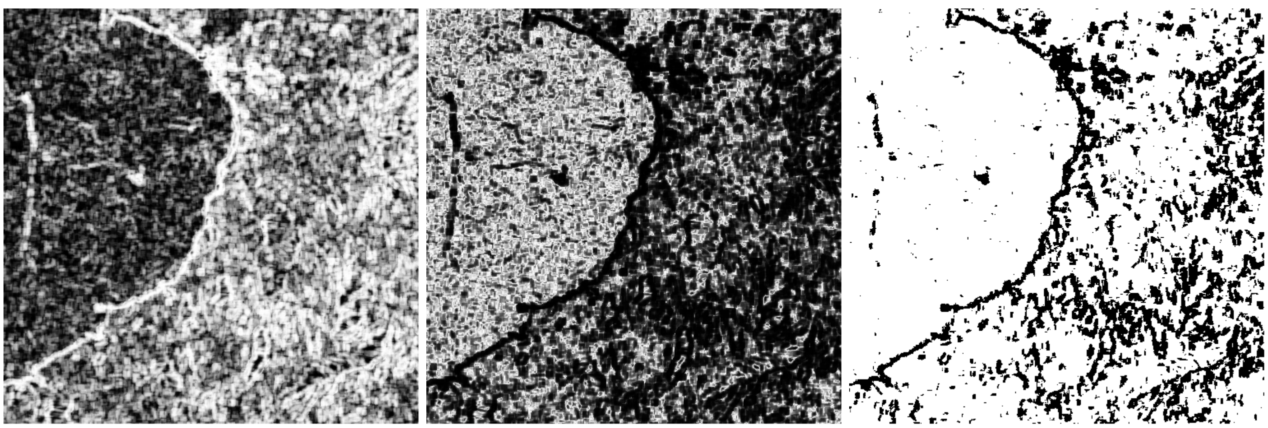

(a) **(b)** **(c)**

Figure 11: Results for a threshold of 0.05 of the p-value, Shannon entropy, $L = 18$.

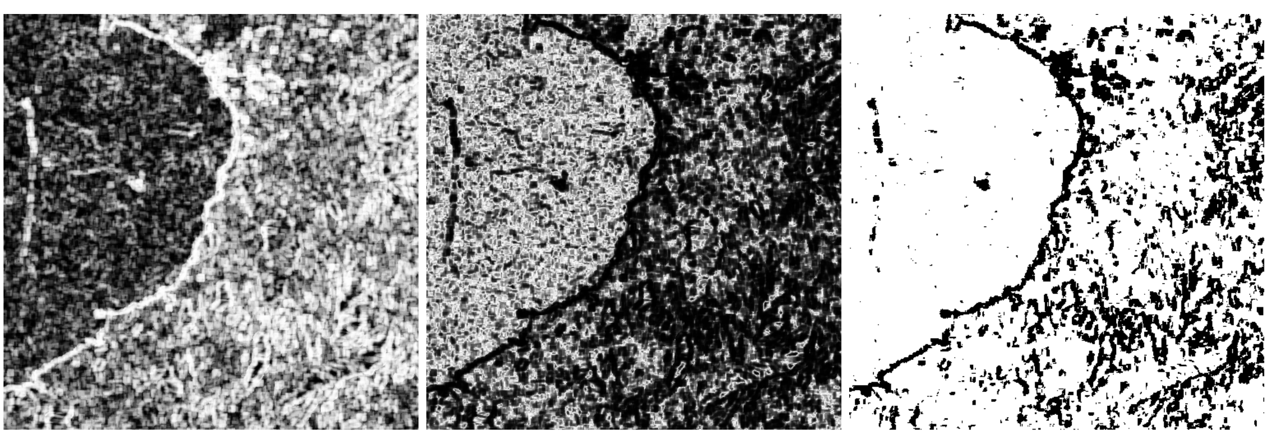

(a) **(b)** **(c)**

Figure 12: Results for a threshold of 0.05 of the p-value, Rényi Entropy, $L = 18$, $\lambda = 0.9$, $n = 49$.

Analysis of Performance

The performance of the proposed methods was evaluated using the Mean Squared Error (MSE) as a global metric to compare the detection accuracy of heterogeneous regions. First, test statistics were computed for both Shannon and Rényi entropy-based approaches across the image using a sliding window of size 7×7. Then, p-values were calculated for each window based on the distribution of the test statistics, assuming a null hypothesis of homogeneity. A significance level of $\alpha = 0.05$ was applied to construct binary maps, where pixels with $p \leq \alpha$ were classified as heterogeneous (value 1), and pixels with $p > \alpha$ were classified as homogeneous (value 0).

The MSE values indicate that the Rényi entropy-based approach outperformed the Shannon entropy-based method, with a lower global MSE (Rényi: 0.1436 vs. Shannon: 0.2066). This result suggests that Rényi entropy captures heterogeneity more effectively. Additionally, local error maps comparing the binary predictions with the ground truth show that the Rényi entropy-based method has fewer misclassifications (errors) across the image, particularly in heterogeneous regions, further supporting its superior performance.

Derivation of the Rényi Entropy for the G_I^0 Distribution

The Rényi entropy of order λ for a continuous random variable Z with density $f_Z(z)$ is given by:

$$H_\lambda(Z) = \frac{1}{1-\lambda} \ln \left(\int_0^\infty [f_Z(z)]^\lambda \, dz \right), \quad \lambda > 0, \, \lambda \neq 1.$$

For $Z \sim G_I^0(\alpha, \gamma, L)$, the density function is:

$$f_Z(z) = C \cdot \frac{z^{L-1}}{(\gamma + Lz)^{L-\alpha}}, \quad \text{where} \quad C = \frac{L^L \Gamma(L-\alpha)}{\gamma^\alpha \Gamma(-\alpha)\Gamma(L)}.$$

Raising $f_Z(z)$ to the power λ and substituting into the entropy integral, we have:

$$I = \int_0^\infty [f_Z(z)]^\lambda \, dz = C^\lambda \int_0^\infty \frac{z^{\lambda(L-1)}}{(\gamma + Lz)^{\lambda(L-\alpha)}} \, dz.$$

Using the substitution $t = \frac{Lz}{\gamma}$, $z = \frac{\gamma t}{L}$, and $dz = \frac{\gamma}{L} \, dt$, we get:

$$I = C^\lambda \cdot \frac{\gamma^{1+\lambda(\alpha-1)}}{L^{1+\lambda(L-1)}} \int_0^\infty \frac{t^{\lambda(L-1)}}{(1+t)^{\lambda(L-\alpha)}} \, dt.$$

This integral is expressed in terms of the Beta function:

$$\int_0^\infty \frac{t^{a-1}}{(1+t)^{a+b}} \, dt = B(a, b), \quad \text{where} \quad a = \lambda(L-1) + 1, \quad b = \lambda(-\alpha + 1) - 1.$$

Thus,

$$I = C^\lambda \cdot \frac{\gamma^{1+\lambda(\alpha-1)}}{L^{1+\lambda(L-1)}} \cdot B(a, b).$$

We simplify the powers of γ and L:

$$\gamma^{1+\lambda(\alpha-1)} = \gamma^{1-\lambda+\lambda\alpha}, \quad L^{1+\lambda(L-1)} = L^{\lambda L + 1 - \lambda}.$$

Substituting $C^\lambda = L^{L\lambda} \gamma^{-\alpha\lambda} \left(\frac{\Gamma(L-\alpha)}{\Gamma(-\alpha)\Gamma(L)} \right)^\lambda$, we obtain:

$$I = \gamma^{1-\lambda} L^{\lambda-1} \left(\frac{\Gamma(L-\alpha)}{\Gamma(-\alpha)\Gamma(L)} \right)^{\lambda} B(a,b).$$

The Rényi entropy is therefore:

$$H_\lambda(Z) = \frac{1}{1-\lambda} \left[\ln \left(\gamma^{1-\lambda} L^{\lambda-1} \left(\frac{\Gamma(L-\alpha)}{\Gamma(-\alpha)\Gamma(L)} \right)^{\lambda} B(a,b) \right) \right].$$

Simplifying:

$$H_\lambda(G_I^0) = \ln \left(\frac{\gamma}{L} \right) + \frac{1}{1-\lambda} \left[\lambda(\ln \Gamma(L-\alpha) - \ln \Gamma(-\alpha) - \ln \Gamma(L)) + \ln B(a,b) \right].$$

Using the Beta function property $\ln B(a,b) = \ln \Gamma(a) + \ln \Gamma(b) - \ln \Gamma(a+b)$, where $a+b = \lambda(L-\alpha)$, we get the final expression:

$$H_\lambda(G_I^0) = \ln \left(\frac{\gamma}{L} \right) + \frac{1}{1-\lambda} \left[\lambda(\ln \Gamma(L-\alpha) - \ln \Gamma(-\alpha) - \ln \Gamma(L)) + \ln \Gamma(a) + \ln \Gamma(b) - \ln \Gamma(\lambda(L-\alpha)) \right].$$

Given that the mean μ is related to γ by:

$$\mu = -\frac{\gamma}{\alpha+1} \quad \Rightarrow \quad \gamma = -\mu(\alpha+1),$$

substituting γ into the entropy expression:

$$\begin{aligned} &H_\lambda(G_I^0) = \ln \left(\frac{-\mu(\alpha+1)}{L} \right) \\ &+ \frac{1}{1-\lambda} \left[\lambda \left(\ln \Gamma(L-\alpha) - \ln \Gamma(-\alpha) - \ln \Gamma(L) \right) + \ln \Gamma\left(\lambda(L-1)+1 \right) + \ln \Gamma\left(\lambda(-\alpha+1)-1 \right) - \ln \Gamma\left(\lambda(L-\alpha) \right) \right]. \end{aligned}$$

Therefore:

$$\begin{aligned} &H_\lambda(G_I^0) = \ln \mu + \ln(-1-\alpha) - \ln L \\ &+ \frac{1}{1-\lambda} \left[\lambda \left(\ln \Gamma(L-\alpha) - \ln \Gamma(-\alpha) - \ln \Gamma(L) \right) + \ln \Gamma\left(\lambda(L-1)+1 \right) + \ln \Gamma\left(\lambda(-\alpha+1)-1 \right) - \ln \Gamma\left(\lambda(L-\alpha) \right) \right]. \end{aligned} \tag{11}$$

Derivation of the Rényi Entropy for the Γ_{SAR} Distribution

To compute the Rényi entropy of $\Gamma_{\text{SAR}}(L,\mu)$, we need to evaluate the integral:

$$I = \int_0^\infty [f_Z(z;L,\mu)]^\lambda \, dz = \left(\frac{L^L}{\Gamma(L)\mu^L} \right)^{\lambda} \int_0^\infty z^{\lambda(L-1)} \, e^{-\lambda L z/\mu} \, dz.$$

This integral can be evaluated using the Gamma integral formula:

$$\int_0^\infty x^{p-1} e^{-qx} \, dx = \frac{\Gamma(p)}{q^p}, \quad \text{for } p>0,\ q>0,$$

where $p = \lambda L - \lambda + 1$ and $q = \frac{\lambda L}{\mu}$. Substituting these values into the integral, we obtain:

$$I = \left(\frac{L^L}{\Gamma(L)\mu^L}\right)^\lambda \frac{\Gamma(\lambda L - \lambda + 1)}{\left(\frac{\lambda L}{\mu}\right)^{\lambda L - \lambda + 1}}.$$

The natural logarithm of the integral is then given by:

$$\ln I = \lambda \left(L \ln L - L \ln \mu - \ln \Gamma(L)\right) + \ln \Gamma(\lambda L - \lambda + 1) - (\lambda L - \lambda + 1)\left(\ln \lambda L - \ln \mu\right).$$

The Rényi entropy $H_\lambda(Z)$ can be computed by substituting $\ln I$ into the definition:

$$H_\lambda(Z) = \frac{1}{1-\lambda} \ln I.$$

Expanding and simplifying the terms, the Rényi entropy of $\Gamma_{\text{SAR}}(L, \mu)$ becomes:

$$H_\lambda(\Gamma_{\text{SAR}}) = \frac{1}{\lambda - 1}\left[\lambda \ln \Gamma(L) - \ln \Gamma\big(\lambda(L-1)+1\big) - (\lambda - 1)\big(\ln L - \ln \mu\big) + \big(\lambda(L-1)+1\big)\ln \lambda\right].$$

References

Argenti, Fabrizio, Alessandro Lapini, Tiziano Bianchi and Luciano Alparone. 2013. "A Tutorial on Speckle Reduction in Synthetic Aperture Radar Images." *IEEE Geoscience and Remote Sensing Magazine* 1(3):6–35.

Avval, Tahereh G., Behnam Moeini, Victoria Carver, Neal Fairley, Emily F. Smith, Jonas Baltrusaitis, Vincent Fernandez, Bonnie. J. Tyler, Neal Gallagher and Matthew R. Linford. 2021. "The Often-Overlooked Power of Summary Statistics in Exploratory Data Analysis: Comparison of Pattern Recognition Entropy (PRE) to Other Summary Statistics and Introduction of Divided Spectrum-PRE (DS-PRE)." *Journal of Chemical Information and Modeling* 61(9):4173–4189.

Cassetti, J., D. Delgadino, A. Rey and A. C. Frery. 2022. "Entropy Estimators in SAR Image Classification." *Entropy* 24(4):509.

De A. Ferreira, J. and Abraao D. C. Nascimento. 2020. "Shannon Entropy for the $\mathcal{G}_I^0$ Model: A New Segmentation Approach." *IEEE Journal of Selected Topics in Applied Earth Observations and Remote Sensing* 13:2547–2553.

Frery, A. C., H.-J. Muller, C.C.F. Yanasse and S.J.S. Sant'Anna. 1997. "A model for extremely heterogeneous clutter." *IEEE Transactions on Geoscience and Remote Sensing* 35(3):648–659.

Michelucci, Umberto and Francesca Venturini. 2021. "Estimating Neural Network's Performance with Bootstrap: A Tutorial." *Machine Learning and Knowledge Extraction* 3(2):357–373.

Mohammad-Djafari, Ali. 2015. "Entropy, Information Theory, Information Geometry and Bayesian Inference in Data, Signal and Image Processing and Inverse Problems." *Entropy* 17(6):3989–4027.

Moreira, Alberto, Pau Prats-Iraola, Marwan Younis, Gerhard Krieger, Irena Hajnsek and Konstantinos P. Papathanassiou. 2013. "A tutorial on synthetic aperture radar." *IEEE Geoscience and Remote Sensing Magazine* 1(1):6–43.

Mu, Y., B. Huang, Z Pan, H. Yang, G. Hou and J. Duan. 2019. "An Enhanced High-Order Variational Model Based on Speckle Noise Removal With G^0 Distribution." *IEEE Access* 7:104365–104379.

Nascimento, A. D. C., R. J. Cintra and A. C. Frery. 2010. "Hypothesis Testing in Speckled Data With Stochastic Distances." *IEEE Transactions on Geoscience and Remote Sensing* 48(1):373–385.

Nascimento, Abraao D. C., Alejandro C. Frery and Renato J. Cintra. 2019. "Detecting Changes in Fully Polarimetric SAR Imagery With Statistical Information Theory." *IEEE Transactions on Geoscience and Remote Sensing* 57(3):1380–1392.

Nascimento, Abraao D. C., Michelle M. Horta, Alejandro C. Frery and Renato J. Cintra. 2014. "Comparing Edge Detection Methods Based on Stochastic Entropies and Distances for PolSAR Imagery." *IEEE Journal of Selected Topics in Applied Earth Observations and Remote Sensing* 7(2):648–663.

Pressé, Steve, Kingshuk Ghosh, Julian Lee and Ken A. Dill. 2013. "Principles of maximum entropy and maximum caliber in statistical physics." *Reviews of Modern Physics* 85(3):1115–1141.

Shannon, C. E. 1948. "A Mathematical Theory of Communication." *The Bell System Technical Journal* 27(3):379–423.